

pubs.acs.org/JPCA Article

# Probing the Dependence of Long-Range, Four-Atom Interactions on Intermolecular Orientation. 4. The Dissociation Dynamics of $H_2/D_2$ ···ICl(B,v'=3) and the Observation of Efficient Vibrational—Rotational Energy Transfer

Published as part of The Journal of Physical Chemistry virtual special issue "Marsha I. Lester Festschrift". Joshua P. Darr\* and Richard A. Loomis\*



Cite This: J. Phys. Chem. A 2022, 126, 7916–7923



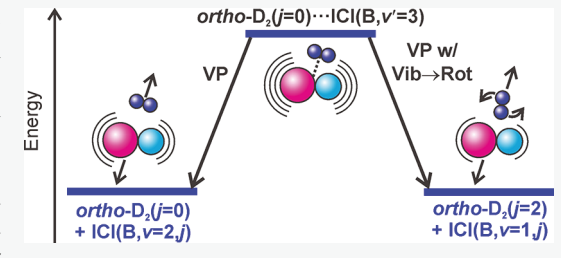
**ACCESS** 

Metrics & More

Article Recommendations

s) Supporting Information

**ABSTRACT:** The vibrational predissociation dynamics of  $H_2/D_2 \cdots I^{35}Cl(B,\nu'=3)$  complexes containing both *para-* and *ortho-*hydrogen prepared in different intermolecular vibrational levels were investigated. The  $\Delta\nu=-1$   $I^{35}Cl(B,\nu=2,j)$  rotational product-state distributions measured for excitation to the lowest-energy T-shaped levels of these complexes are mostly bimodal. The rotational distributions measured for excitation of the  $H_2 \cdots I^{35}Cl(B,\nu'=3)$  complexes are colder than those of the  $D_2 \cdots I^{35}Cl(B,\nu'=3)$  complexes, and there are only slight differences between those measured for the *para-* and *ortho-*hydrogen containing complexes. Excitation of the delocalized bending



levels results in slightly colder rotational product-state distributions. The distributions suggest the dynamics result from more than impulsive dissociation off of the inner repulsive wall of the lower-energy  $H_2/D_2 + I^{35}Cl(B_1v = 2)$  potential surfaces of the products. The depths of these potentials and the energies available to these products also contribute to the dynamics. The formation of the  $\Delta v = -2$ ,  $I^{35}Cl(B_1v = 1)$  product channel was only identified for excitation of levels within the ortho(j = 0)- $D_2 + I^{35}Cl(B_1v'=3)$  potential. The formation of this channel occurs via  $I^{35}Cl(B_1v'=3)$  vibrational to  $D_2$  rotational energy transfer forming the ortho(j = 2)- $D_2 + I^{35}Cl(B_1v'=3)$  products.

# INTRODUCTION

Rare gas-dihalogen (Rg···XY) van der Waals complexes have been extensively studied over the last 45 years as a means to investigate unimolecular reaction dynamics, energy transfer mechanisms, and intermolecular forces. 1-3 In part because of their strong absorption throughout the visible and ultraviolet regions and the relative simplicity of these three-atom systems, the Rg...XY complexes are well suited for both experimental and theoretical efforts, and accurate depictions of the chemical physics continue to be established. The vibrational predissociation (VP) dynamics of Rg...XY complexes, in particular, have been utilized to investigate vibrational to rotational energy transfer dynamics. Following vibronic photoexcitation of the XY moiety, XY vibrational energy is transferred to the intermolecular coordinate, and the complex dissociates into separate Rg and XY products, where the electronically excited XY molecule has less vibrational excitation and varying amounts of rotational excitation.

Lester and co-workers performed some of the seminal work in these efforts, measuring the ICl(A,v,j) and ICl(B,v,j) rotational product-state distributions formed via VP of the T-shaped Ne··· ICl(A,v'), He···ICl(B,v'), and Ne···ICl(B,v') heteronuclear dihalogen complexes.<sup>4–7</sup> Unlike those measured for some

homonuclear Rg···X<sub>2</sub> complexes, <sup>8</sup> the ICl(A,v,j) and ICl(B,v,j)rotational product-state distributions were found to be bimodal with two distinct maxima, referred to as rotational rainbows. These rotational distributions were attributed to contrasting impulsive, half-collision intermolecular forces between the Rg atom and ICl molecule experienced along varying angular regions of the anisotropic repulsive region of the lower-energy potential energy surface (PES). We previously extended these Rg...XY VP investigations using transitions of the T-shaped and linear, ground-state He···ICl( $X,\nu''=0$ ) conformers to access  $He\cdots ICl(B,v',n')$  intermolecular vibrational levels with varying amounts of intermolecular bending excitation, which sample wider angular regions of the intermolecular PES. 9,10 The rotational product-state distributions measured for these bending levels were slightly colder, and the dynamics were associated with impulsive scattering from the inner repulsive

Received: August 13, 2022 Revised: October 10, 2022 Published: October 25, 2022





wall of the He +  $ICl(B,\nu'-1)$  PES and little interaction with the attractive well of that PES.

We previously reported on the spectroscopy, intermolecular interactions, and energetics of the four-atom, H<sub>2</sub>/D<sub>2</sub>···ICl and  $H_2/D_2\cdots I_2$  dihalogen systems including the *para-* and *ortho*-hydrogen and deuterium molecules. Unless otherwise indicated, para-H<sub>2</sub> and ortho-H<sub>2</sub> are the j = 0 and j = 1 H<sub>2</sub> rotational states without vibrational or electronic excitation, and they are abbreviated as p-H<sub>2</sub> and o-H<sub>2</sub>, respectively. Similarly, the j = 0 and j = 1 rotational states of  $D_2$  are abbreviated as o- $D_2$ and p- $D_{2}$ , respectively. In that work,  $^{11-13}$  we found there are at least two distinct ground-state  $p,o-H_2/D_2\cdots XY(X,v''=0)$  conformers, one with the H<sub>2</sub>/D<sub>2</sub> moiety localized along the dihalogen bond axis, which is labeled the linear complex, and one with the H<sub>2</sub>/D<sub>2</sub> subunit positioned perpendicularly to the dihalogen bond axis, which is termed the T-shaped complex. This is analogous to the ground-state linear and T-shaped conformers, respectively, that were reported for several Rg···XY van der Waals complexes. <sup>10,14–19</sup> The p,o-H<sub>2</sub>/D<sub>2</sub>···XY(B, $\nu'$ ,n') excited-state levels accessed by the transitions of the different  $p,o-H_2/D_2\cdots XY(X,v''=0)$  conformers 11-13 are analogous to the Rg...XY complexes. The prominent spectral feature of the Tshaped conformer for each complex was assigned as accessing the n' = 0 lowest-energy intermolecular vibrational level in the excited state, which also has a T-shaped geometry. Multiple features of the linear conformer were also observed. A series of lower-energy transitions was assigned as accessing bending levels with the H<sub>2</sub>/D<sub>2</sub> moiety delocalized along the angular coordinate. Transitions at even higher energies were assigned through comparison with theory as accessing levels with both intermolecular stretching and bending excitation. 11-13

The prominent dissociation mechanism of the  $p,o\text{-}\mathrm{H}_2/\mathrm{D}_2\cdots$  ICl( $B,\nu'=3$ ) complexes is VP, as was shown for numerous Rg··· ICl( $B,\nu'=2,3$ ) complexes. The crossing of multiple repulsive curves near the ICl( $B,\nu'=3$ ) molecular level results in the excited-state lifetimes shortening from ~5  $\mu$ s for the ICl( $B,\nu'=1,2$ ) levels down to <200 ps due to electronic predissociation. Despite this, spectral features are observed in laser-induced fluorescence (LIF) spectra because of the high efficiency for VP of the Rg···ICl( $B,\nu'=3$ ) and  $p,o\text{-}\mathrm{H}_2/\mathrm{D}_2\cdots$  ICl( $B,\nu'=3$ ) complexes, and the formation of ICl( $B,\nu<3$ ) products that then relax via spontaneous emission. Intramolecular vibrational energy redistribution (IVR) does not occur for the  $p,o\text{-}\mathrm{H}_2/\mathrm{D}_2\cdots \mathrm{I}^{35}\mathrm{Cl}(B,\nu')$  complexes as their binding energies are not large enough to couple with levels bound within the lower-lying PESs.

The VP dynamics of the  $p_1o-H_2/D_2\cdots ICl(B_1v'=3)$  systems offer multiple interactions that warrant the investigation of their inelastic half-collision dissociation dynamics, and we describe those in this paper. The numerous intermolecular vibrational levels bound within the  $p_1o-H_2/D_2 + ICl(B_1v'=3)$  PES permit complexes with different available energies and that sample varying regions of that PES to be investigated. The H<sub>2</sub> and D<sub>2</sub> moieties have para and ortho states, and the complexes containing each have contrasting binding energies. The results obtained from the o,p-D<sub>2</sub>···ICl complexes can be compared with the published results on the isobaric He···ICl complex, which has a smaller binding energy, to probe the role of available energy and the well depth of the lower-energy PES of the products on the dissociation dynamics. Finally, the four-atom p,o-H<sub>2</sub>/D<sub>2</sub>···ICl systems offer the pathway of ICl vibrational energy to H<sub>2</sub>/D<sub>2</sub> rotational energy transfer, which the threeatom Rg…XY systems do not have.

#### EXPERIMENTAL SECTION

The stabilization of the ground-state  $p_1o-H_2/D_2\cdots I^{35}Cl(X_1\nu''=0)$ complexes was performed in the same manner described previously.  $^{11,12}$  A 5–10%  $H_2$  in He or  $D_2$  in He carrier gas was passed through a vessel containing solid ICl at 274 K. The gas mixture was pressurized to 5930 Torr and expanded through a pulsed valve with an 0.89 mm diameter orifice into a vacuum chamber held at pressures < 20 mTorr. The dissociation dynamics experiments were performed using frequency-resolved two-color, pump-probe spectroscopy in the same manner as described for the  $\text{He} \cdot \cdot \cdot \text{I}^{35}\text{Cl}(B_1 v' = 3_1 n')$  studies. The photon energy of a nanosecond dye laser was fixed on the most intense peak within the feature associated with transitions from the ground-state T-shaped or linear  $p,o-H_2/D_2\cdots I^{35}Cl(X,v''=0)$ conformers to a specific  $p,o-H_2/D_2\cdots I^{35}Cl(B,v'=3,n')$  excitedstate level. These transition energies, the excited-state intermolecular vibrational level, n', assigned for each transition, which was largely based on comparison with theory, and the binding energies of the levels below the dissociation asymptote were reported previously 11,12 and are summarized in Table 1. Data for the He···I<sup>35</sup>Cl complex<sup>9,24</sup> are also included as comparisons will be made to the distributions measured for those levels.

Table 1. Summary of the Complexes, the n' Levels Accessed, Their Binding Energies (in cm $^{-1}$ ) within the p,o- $H_2/D_2+I^{35}Cl(B,\nu'=3)$  and  $He+I^{35}Cl(B,\nu'=3)$  PESs, the Pump Transition Energies (in cm $^{-1}$ ), and the Ground-State  $H_2/D_2/He$ ··· $I^{35}Cl(X,\nu''=0)$  Conformers Used in These Transitions  $^{9,11,12,24}$ 

comple	x n'	binding energy	transition energy	conformer
p-H <sub>2</sub> ···I <sup>35</sup>	<sup>5</sup> Cl 0	59.4-67.3	17 838.2	T-shaped
o-H <sub>2</sub> ···I <sup>35</sup>	<sup>5</sup> Cl 0	69.5-76.3	17 841.1	T-shaped
$p$ - $H_2$ ··· $I^{35}$	<sup>5</sup> Cl 3	43.3(1.3)	17 941.0	Linear
o-H <sub>2</sub> ····I <sup>35</sup>	<sup>5</sup> Cl 3	46.1(3)	17 967.8	Linear
o-H <sub>2</sub> ····I <sup>35</sup>	<sup>5</sup> Cl ∼10	7.9(3)	18 006.0	Linear
$o$ - $D_2$ ··· $I^{35}$	Cl 0	75.3-82.8	17 839.9	T-shaped
$p-D_2 \cdots I^{35}$	<sup>5</sup> Cl 0	80.7-87.3	17 844.1	T-shaped
o-D <sub>2</sub> I <sup>35</sup>	Cl 3	53(2)	17 976.4	Linear
$p$ - $D_2$ ··· $I^{35}$	<sup>5</sup> Cl 3	56.0(2.4)	17 995.4	Linear
He…I <sup>35</sup> C	0 0	13.3(3)	17 830.80	T-shaped
He…I <sup>35</sup> C	2 2	7.6(2)	17 841.73	Linear
He…I <sup>35</sup> C	21 3	6.4(2)	17 842.87	Linear

A second nanosecond dye laser was delayed by ~15 ns from the pump laser and intersected the expansion at the same position as the pump laser, ~10 mm downstream from the exit of the pulsed valve. Most of the I<sup>35</sup>Cl(B, $\nu$  = 2,j) rotational product spectra were recorded by scanning the wavenumber of the probe laser across the I<sup>35</sup>Cl(E, $\nu$ <sup>†</sup>) ion-pair state was preferentially collected using a UG-1 filter and imaged onto a UV-sensitive PMT. The short-lived ICl ion-pair state fluorescence was collected with a boxcar integrator (~40 ns gate width). Several product spectra were recorded consecutively under identical conditions, and these were averaged and calibrated using known spectroscopic parameters for I<sup>35</sup>Cl.<sup>25–27</sup>

The probe spectra of the  $I^{35}Cl(B,\nu)$  products were overlapped by known  $I^{35}Cl(\beta-A,\nu^{\dagger}-\nu$  transitions. <sup>25,26</sup> As shown for several Rg···XY complexes, <sup>11-13,18,19,28-31</sup> excitation of the linear H<sub>2</sub>/D<sub>2</sub>··· $I^{35}Cl(X,\nu''=0)$  or He··· $I^{35}Cl(X,\nu''=0)$  complexes to the continuum of states lying above the asymptotes of the H<sub>2</sub>/D<sub>2</sub> +

 $I^{35}Cl(A,\nu')$  or He +  $I^{35}Cl(A,\nu')$  intermolecular PESs results in prompt direct dissociation and the formation of  $H_2/D_2$  or He +  $I^{35}Cl(A,\nu')$  products. Some of the  $I^{35}Cl(B,\nu')$  product spectra were weak, and the overlapping  $I^{35}Cl(B,\nu')$  product spectra prohibited a straightforward determination of the  $I^{35}Cl(B,\nu,j)$  rotational product-state distribution. In these circumstances, an  $I^{35}Cl(B,-A,\nu^{\dagger}-\nu)$  background probe spectrum was collected by tuning the pump laser just off of the transition to the desired  $p,o-H_2/D_2\cdots I^{35}Cl(B,\nu'=3,n')$  intermolecular level to where only the continuum transitions are present. This  $I^{35}Cl(B,-A,\nu^{\dagger}-\nu')$  background spectrum was then subtracted from the spectrum collected by exciting the  $p,o-H_2/D_2\cdots I^{35}Cl(B,\nu'=3,n')$  intermolecular vibrational level to yield the product spectrum of interest. An example of this background spectrum subtraction is provided in Figure S1 in Supporting Information.

The analyses of the  $I^{35}Cl(B,\nu=2,j)$  rotational product-state distributions were performed in the same manner as described for the He···ICl investigations. The  $I^{35}Cl(B,\nu=2,j)$  product-state spectrum was fit using a Lorentzian line shape for each transition within the rotational contour to obtain the rotational-product state distribution, see Figure S2 in the Supporting Information for an example fit. Appropriate checks were performed to ensure each spectrum was not affected by saturation or rotational-energy transfer associated with collisions. To prevent the former, probe pulse energies  $\leq 50~\mu J$  were used. Contributions from collisional effects were found to be negligible and certainly less than the error bars of the populations.

# ■ RESULTS AND DISCUSSION

The  $p,o-H_2\cdots I^{35}Cl(B,v'=3,n')$  intermolecular vibrational levels accessed throughout the ICl B-X, 3-0 spectral region undergo VP to form  $p,o-H_2 + I^{35}Cl(B,v = 2,j)$   $\Delta v = -1$  products, as reported previously.<sup>11</sup> In order to better characterize the contrasting VP dynamics incurred from the different p,o-H<sub>2</sub>/  $D_2 \cdots I^{35}Cl(B, \nu'=3, n')$  intermolecular vibrational levels and the regions of the excited-state PES sampled, we present herein the  $I^{35}Cl(B, \nu = 2, j)$  VP product spectra recorded following excitation to each level; illustrative  $I^{35}Cl(B, \nu = 2, j)$  product spectra are presented in Figure 1. Each spectrum contains overlapping P(j) and R(j) spectral lines with a maximum intensity at the R-bandhead, followed by a weak secondary maximum and a gradual decay in intensity of the rotational lines extending to lower wavenumbers. The product spectra measured when exciting the p- and o-containing complexes for each system are quite similar. The product spectra for the o,p- $D_2 \cdots I^{35}Cl(B_{\nu}'=3)$  complexes appear to be slightly warmer than measured for the  $p,o-H_2\cdots I^{35}Cl(B,\nu'=3)$  complexes. The product spectra recorded with excitation to the n' = 3 delocalized bending levels within the  $p_1o-H_2 + I^{35}Cl(B_1v'=3)$  and  $o_1p-D_2 + I^{35}Cl(B_1v'=3)$  $I^{35}Cl(B,\nu'=3)$  PESs, Figures 1b, d, are appreciably colder than measured for excitation of the T-shaped n' = 0 levels, Figure 1a,

The I<sup>35</sup>Cl(B, $\nu = 2$ ,j) rotational product-state distributions obtained with excitation of the T-shaped p,o-H<sub>2</sub>···I<sup>35</sup>Cl-(B, $\nu'=3$ ,n'=0) levels, Figure 2a, b, are remarkably similar. These distributions are bimodal with a global maximum at j=3 and a secondary local maximum at j=11 in each, and population is observed up to  $j_{\text{max}}=20$  and 19. The distribution for the p-H<sub>2</sub>···I<sup>35</sup>Cl(B, $\nu'=3$ ,n'=3) level is plotted in Figure 2c. This level is 16–24 cm<sup>-1</sup> above the T-shaped n'=0 level, and the p-H<sub>2</sub> moiety is calculated to be delocalized along the angular coordinate about the ICl molecule. <sup>11</sup> The measured distribution

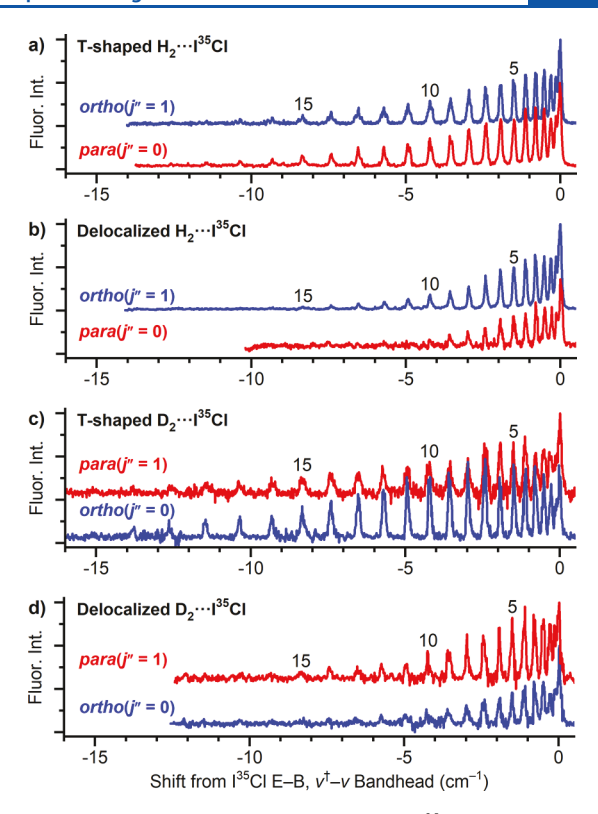


**Figure 1.** Product-state spectra of the  $\Delta \nu = -1$  I<sup>35</sup>Cl(B, $\nu = 2$ ) channel recorded with excitation of the p,o-H<sub>2</sub>···I<sup>35</sup>Cl and o,p-D<sub>2</sub>···I<sup>35</sup>Cl complexes in the ICl B–X, 3–0 region to different intermolecular vibrational levels. The energy axis is relative to the R(j) bandhead in each spectrum. The rotational quantum numbers, j, of several P(j) lines are labeled above the corresponding lines.

is significantly colder than measured for the T-shaped levels with a quick rise and prompt decay in population with  $j_{max} = 12$ , and there is no obvious secondary maximum. In contrast, the distribution for excitation of the delocalized o-H2···I<sup>35</sup>Cl- $(B_{\nu}'=3,n'=3)$  level, which is 24–30 cm<sup>-1</sup> above the n'=0level, solid blue data in Figure 2d, is similar to that measured for the T-shaped n' = 0 level though slightly colder. The  $I^{35}Cl(B_{\nu} =$ 2,j) product-state distribution for an even higher-energy delocalized o-H<sub>2</sub>···I<sup>35</sup>Cl(B, $\nu'$ =3) level was also measured. This level was accessed with a pump photon energy of 18 006 cm<sup>-1</sup>, lying  $62-68 \text{ cm}^{-1}$  above the n'=0 level, and it was tentatively assigned as accessing the n' = 10 delocalized bending level that also has one quantum of intermolecular stretching excitation. The distribution for this level, open circles in Figure 2d, is nearly identical to that of the lower-energy  $o-H_2 \cdots I^{35}Cl(B, \nu'=3, n'=3)$ bending level. Overall, the  $\Delta v = -1 \text{ I}^{35}\text{Cl}(B,v=2)$  rotational product-state distributions that result from the VP of the p,o- $H_2 \cdots I^{35}Cl(B, \nu'=3, n')$  levels are quite similar, with that measured for the delocalized  $p-H_2\cdots I^{35}Cl(B_1v'=3,n'=3)$  level lacking a definitive bimodal structure.

The  $\Delta \nu = -1$  I<sup>35</sup>Cl(B, $\nu = 2$ ,j) rotational product-state distributions were used to calculate the average amount of rotational excitation in the I<sup>35</sup>Cl products,  $\langle E_{\rm rot} \rangle$ , and these are included in Table 2. The energies of the n' intermolecular vibrational levels above the  $\Delta \nu = -1$  p,o-H<sub>2</sub> + I<sup>35</sup>Cl(B, $\nu = 2$ ,j = 0) asymptotes are the amounts of energy available for rotational excitation,  $E_{\rm avail}$ , and these were used to calculate the percent of the  $\langle E_{\rm rot} \rangle$  out of the energy available,  $\langle E_{\rm rot} \rangle / E_{\rm avail}$ . The energy of the highest-energy occupied I<sup>35</sup>Cl(B, $\nu = 2$ ,j) rotational product state,  $E_{\rm max}$ , and the percent of this rotational excitation out of the

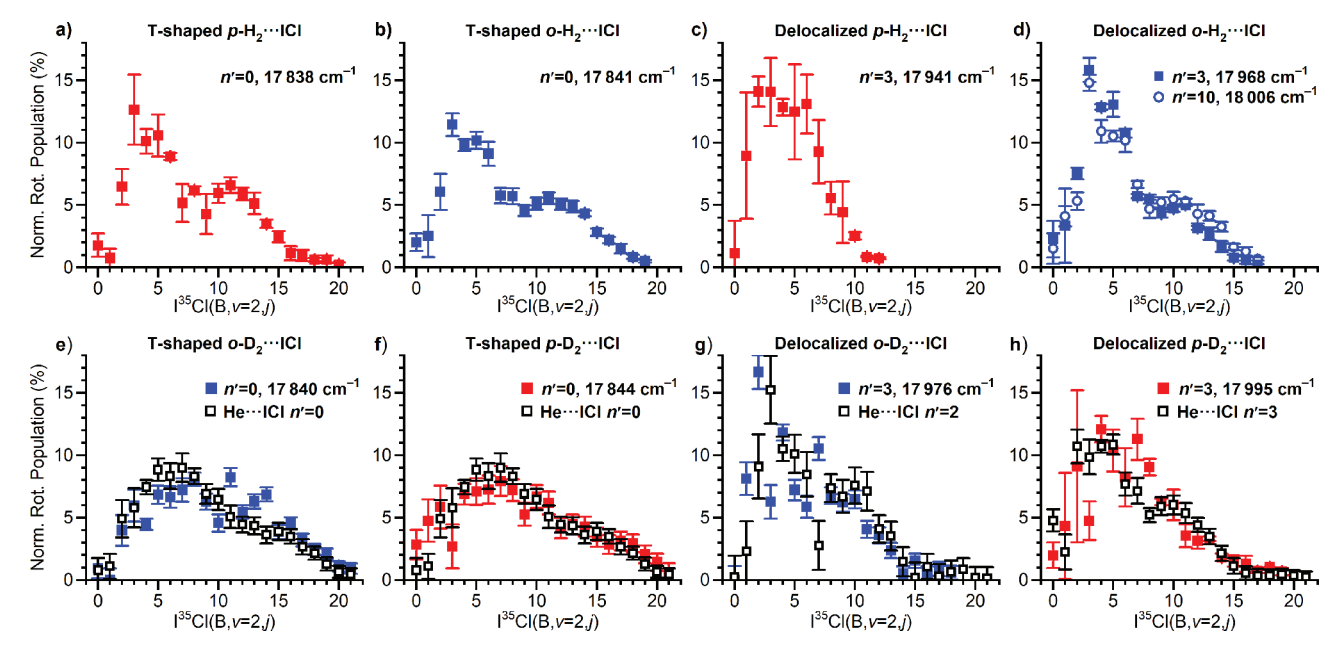


Figure 2.  $\Delta \nu = -1$ ,  $I^{35}Cl(B,\nu = 2,j)$  rotational product-state distributions measured following excitation to numerous p,o- $H_2$ ··· $I^{35}Cl(B,\nu'=3)$  and o,p- $D_2$ ··· $I^{35}Cl(B,\nu'=3)$  intermolecular vibrational levels, shown as solid squares. The distributions measured for excitation of several He··· $I^{35}Cl(B,\nu'=3)$  levels are included in (e)–(h) as open squares. Descriptors of the levels accessed and the transition energies are included.

Table 2. Rotational Energy in the  $\Delta v = -1 \text{ I}^{35}\text{Cl}(B, v = 2)$  Products Formed by the Dissociation of  $\text{H}_2/\text{D}_2$ ···· $\text{I}^{35}\text{Cl}(B, v' = 3, n')$  and  $\text{He}\text{····}\text{I}^{35}\text{Cl}(B, v' = 3, n')^9$  Intermolecular Vibrational Levels<sup>a</sup>

complex	n'	$E_{\rm avail}~({\rm cm}^{-1})$	$\langle E_{\rm rot} \rangle \ ({\rm cm}^{-1})$	$\langle E_{\rm rot} \rangle / E_{\rm avail} $ (%)	$E_{\rm max}~({\rm cm}^{-1})$	$E_{\rm max}/E_{\rm avail}$ (%)
p-H <sub>2</sub> ···I <sup>35</sup> Cl	0	96.1-104.3	6.7(3)	6.4-7.0	34.8	33-36
o-H₂···I³5Cl	0	82.9-89.7	6.9(1)	7.7-8.3	31.5	35-38
$p$ - $H_2$ ··· $I^{35}$ Cl	3	120.1	2.7(5)	2.3	12.9	11
o-H₂···I³⁵Cl	3	117.3	4.4(2)	3.8	25.4	22
o-H₂···I³⁵Cl	~10	155.5	5.58(2)	3.6	25.4	16
o-D₂···I <sup>35</sup> Cl	0	80.1-87.6	10.7(4)	12-13	38.3	44-48
p-D <sub>2</sub> ···I <sup>35</sup> Cl	0	75.6-82.2	9.4(3)	11-12	38.3	47-51
o-D <sub>2</sub> ···I <sup>35</sup> Cl	3	107.4	4.9(3)	4.5	28.4	26
p-D <sub>2</sub> ····I <sup>35</sup> Cl	3	110.	5.7(4)	5.1	31.5	29
He…I <sup>35</sup> Cl	0	150.1	8.4(3)	5.6	38.3	26
He…I <sup>35</sup> Cl	2	156.1	5.7(5)	3.7	38.3	25
He…I <sup>35</sup> Cl	3	157.5	5.5(3)	3.5	38.3	24

<sup>a</sup>The available energy,  $E_{\text{avail}}$ , is the energy from the n' level above the  $H_2/D_2/\text{He} + I^{35}\text{Cl}(B,\nu-2,j=0)$  asymptotes. The average amount of rotational excitation,  $\langle E_{\text{rot}} \rangle$ ,  $\langle E_{\text{rot}} \rangle / E_{\text{avail}}$  the maximum rotational energy,  $E_{\text{max}}$  and  $E_{\text{max}}/E_{\text{avail}}$  are included.

maximum energy available for the I<sup>35</sup>Cl(B, $\nu$  = 2) products,  $E_{\rm max}/E_{\rm avail}$ , are also included.

The amounts of  $\langle E_{\rm rot} \rangle$  formed by the VP of the rigidly T-shaped p-H<sub>2</sub>···I<sup>35</sup>Cl(B, $\nu'$ =3,n'=0) and o-H<sub>2</sub>···I<sup>35</sup>Cl(B, $\nu'$ =3,n'=0) levels are 6.7 and 6.9 cm<sup>-1</sup>, which represent  $\langle E_{\rm rot} \rangle / E_{\rm avail} = 6.4$ –7.0% and 7.7–8.3%, respectively. The excitation to the n'=3, higher-energy intermolecular vibrational level with the H<sub>2</sub> moiety more delocalized about the I<sup>35</sup>Cl molecule results in rotationally colder I<sup>35</sup>Cl(B, $\nu$ =2,j) distributions with  $\langle E_{\rm rot} \rangle = 2.7$  and 4.4 cm<sup>-1</sup> and just  $\langle E_{\rm rot} \rangle / E_{\rm avail} = 2.3\%$  and 3.8% for the p-H<sub>2</sub>··· I<sup>35</sup>Cl(B, $\nu'$ =3,n'=3) and o-H<sub>2</sub>···I<sup>35</sup>Cl(B, $\nu'$ =3,n'=3) complexes, respectively. The  $\langle E_{\rm rot} \rangle$  increases slightly although  $\langle E_{\rm rot} \rangle / E_{\rm avail}$  decreases slightly, 5.58 cm<sup>-1</sup> and 3.6%, when exciting the o-H<sub>2</sub>··· I<sup>35</sup>Cl(B, $\nu'$ =3,n' ~ 10) level, which is predicted to have both intermolecular bending and stretching excitation and is 38.2 cm<sup>-1</sup> to higher energy than the n'=3 level.

The larger mass of  $D_2$  versus  $H_2$  results in lower zero-point energies for the  $o_1p$ - $D_2$ ··· $I^{35}$ Cl( $B_1\nu'=3$ ) complexes. Consequently, the amount of  $E_{avail}$  for the  $\Delta\nu=-1$  VP products is

lower for the  $D_2$  complexes than for the  $H_2$  complexes. The  $\Delta \nu =$  $-1 I^{35}Cl(B_{\nu} = 2_{ij})$  rotational product-state distributions measured following excitation of the T-shaped o,p-D2···I<sup>35</sup>Cl-(B,v'=3,n'=0) levels, Figure 2e, f, are quite similar, and they are slightly bimodal with maxima near j = 8 and 14. These distributions are warmer, with  $\langle E_{\text{rot}} \rangle = 10.7$  and 9.4 cm<sup>-1</sup> and  $\langle E_{\rm rot} \rangle / E_{\rm avail} = 12-13\%$  and 11-12%, respectively, than those measured for excitation of the  $p,o-H_2\cdots I^{35}Cl(B,v'=3,n'=0)$  levels. The distributions obtained when exciting the o,p-D<sub>2</sub>···I<sup>35</sup>Cl- $(B_1v'=3,n'=3)$  levels with intermolecular bending excitation sufficient for sampling the linear regions of the intermolecular PES, shown in Figure 2g, h, are rotationally colder than the n' = 0distributions with  $\langle E_{\rm rot} \rangle$  = 4.9 and 5.7 cm<sup>-1</sup> and  $\langle E_{\rm rot} \rangle / E_{\rm avail}$  = 4.5% and 5.1%, respectively. Just as with excitation of the Tshaped levels, the distributions for exciting the o,p-D2...  $I^{35}Cl(B,\nu'=3,n'=3)$  bending levels are warmer than those measured for the  $p,o-H_2\cdots I^{35}Cl(B,v'=3,n'=3)$  bending levels.

Calculations of the excitation spectra and the nature of the excited-state intermolecular vibrational levels accessed were

performed on numerous systems, including He···ICl(B, $\nu'$ ), <sup>20,32</sup> He···Br<sub>2</sub>(B, $\nu'$ ), <sup>14</sup> He···I<sub>2</sub>(B, $\nu'$ ), <sup>18</sup> H<sub>2</sub>/D<sub>2</sub>···I<sub>2</sub>(B, $\nu'$ ), <sup>13</sup> H<sub>2</sub>···ICl(B, $\nu'$ ), <sup>11</sup> and D<sub>2</sub>···ICl(B, $\nu'$ ). <sup>12</sup> The calculations indicate the rovibronic spectra are not very sensitive to the details of the PES as long as the potential minimum and the barriers to internal rotation are approximately correct. The agreement may also indicate the anisotropies of these PESs are rather similar, being dictated by the dihalogen moiety. Furthermore, it was found in the four-atom systems that near quantitative agreement with the experimental spectra could be achieved treating the p-H2 and o- $\mathrm{D}_2$  molecules as spheres with the appropriate masses.  $^{11-13}$ These reports led us to compare the  $I^{35}Cl(B, \nu = 2, j)$  rotational product-state distributions measured for excitation to the Tshaped and delocalized levels bound within the o,p-D2 +  $I^{35}Cl(B,\nu'=3)$  and the isobaric He +  $I^{35}Cl(B,\nu'=3)$  PES. The goal here was to identify contributions from  $E_{\mathrm{avail}}$  and the attractive regions of the lower-energy  $o,p-D_2/He + I^{35}Cl(B,v=2)$  PESs of the products on the VP dynamics.

The  $I^{35}Cl(B,\nu,j)$  rotational product-state distributions measured with excitation of numerous levels bound within the He +  $I^{35}Cl(B,\nu'=2,3)$  PESs were published previously. The rotational product-state distribution measured with excitation of the rigidly T-shaped He···I<sup>35</sup>Cl(B, $\nu'$ =3,n'=0) level, open squares in Figures 2e, is slightly different than measured for the o-D<sub>2</sub>···I<sup>35</sup>Cl-(B,v'=3,n'=0) level with a less-obvious bimodal structure and a lower value of  $\langle E_{\rm rot} \rangle$ , 8.4 cm<sup>-1</sup> versus 10.7 cm<sup>-1</sup>. The significantly smaller binding energy for the T-shaped He···  $I^{35}Cl(B,\nu'=3,n'=0)$  complex also results in  $\langle E_{rot}\rangle/E_{avail}$  being more than  $2\times$  smaller for the He complex than for the o-D<sub>2</sub>...  $I^{35}Cl(B,\nu'=3,n'=0)$  complex, 5.6% versus 12–13%. The distributions for excitation of the T-shaped He···I<sup>35</sup>Cl- $(B, \nu' = 3, n' = 0)$  and  $p-D_2 \cdots I^{35}Cl(B, \nu' = 3, n' = 0)$  levels are nearly the same, as indicated in Figure 2f, with the distribution of the four-atom complex being only slightly warmer. The product distributions for the  $o_1p$ - $D_2$ ···I<sup>35</sup>Cl(B<sub>1</sub>v'=3,n'=3) bending levels are quite similar to those of the n' = 2 and n' = 3 bending levels of the He···I<sup>35</sup>Cl(B, $\nu'$ =3) complexes although quantitative comparison is difficult due to the uncertainties in the populations measured for the four-atom complexes. Some of the subtle differences could be due to the specific rotational states of the excited-state complexes that are accessed; these experiments were conducted with excitation of the most intense peak of each complex feature, and the excitation of slightly different rotational states likely results in contrasting rotational product-state

The  $I^{35}Cl(B, v = 2,j)$  rotational product-state distributions measured after exciting the rigidly T-shaped n' = 0 levels are the coldest for  $p,o-H_2\cdots I^{35}Cl(B,v'=3)$  and the warmest for  $o,p-D_2\cdots$  $I^{35}Cl(B,\nu'=3)$ , as indicated in Table 2. The simplistic calculations of the excited-state PESs,  $^{11,12,32}$  and the agreement of the calculated excitation spectra with the experimental spectra of these complexes suggest the anisotropies of these surfaces are likely quite similar. The calculated probability amplitudes for the rigidly, T-shaped n' = 0 and the low-lying bending n' = 3 levels for all of these complexes sample nearly the same regions of their intermolecular PESs. 11,12,32 Ultimately, the anisotropies of the PESs sampled immediately following VP and the impulsive dissociation off of the steep, repulsive potential wall at small internuclear separations, R, likely contribute to the bimodal nature of the  $\Delta v = -1 \text{ I}^{35}\text{Cl}(B, v = 2, j)$  rotational product-state distributions. But, we propose there are two additional contributions to the VP dynamics incurred and the productstate distributions measured: the amount of  $E_{\text{avail}}$  in comparison

to the well depth of the  $\Delta v = -1$  intermolecular PES and the masses of the constituents within each complex.

The first contribution was presented by Nejad-Sattari and Stephenson in interpreting the VP dynamics of Ne···Br<sub>2</sub>. 33 Specifically, they concluded that when  $E_{\text{avail}}$  is small relative to the well depth,  $D_e$ , of the lower-energy PES of the products, the more anisotropic, attractive well region of that PES will largely dictate the dynamics of the products out the exit channel. The binding energies of the T-shaped  $o,p-D_2\cdots I^{35}Cl(B,v'=3,n'=0)$ levels are larger than those of the  $p,o-H_2\cdots I^{35}Cl(B,v'=3,n'=0)$ levels, and these are significantly larger than those of the threeatom T-shaped He···I<sup>35</sup>Cl(B, $\nu'=3,n'=0$ ) complexes, as indicated in Table 1. All of these complexes undergo VP on fast time scales accessing the inner repulsive walls of the lower-energy PESs associated with the I<sup>35</sup>Cl(B, $\nu = 2,j$ ) products. The amounts of  $E_{\text{avail}}$  for the dissociating products are determined by the binding energies of the n' = 0 levels, and the  $o,p-D_2 + I^{35}Cl(B,v = 2,j)$ product pairs have the smallest  $E_{\text{avail}}$ , ~ 84 cm<sup>-1</sup> and ~79 cm<sup>-1</sup> for the o-D2- and p-D2-containing complexes, and the He +

I<sup>35</sup>Cl(B, $\nu = 2,j$ ) products have the largest  $E_{\text{avail}} \sim 150 \text{ cm}^{-1}$ . The contrasting energetics of the o-D<sub>2</sub>···I<sup>35</sup>Cl(B, $\nu'=3,n'=0$ ) and He···I<sup>35</sup>Cl(B, $\nu'=3,n'=0$ ) complexes are illustrated in Figure 3. The smaller amount of  $E_{\text{avail}}$  for the complexes prepared in the

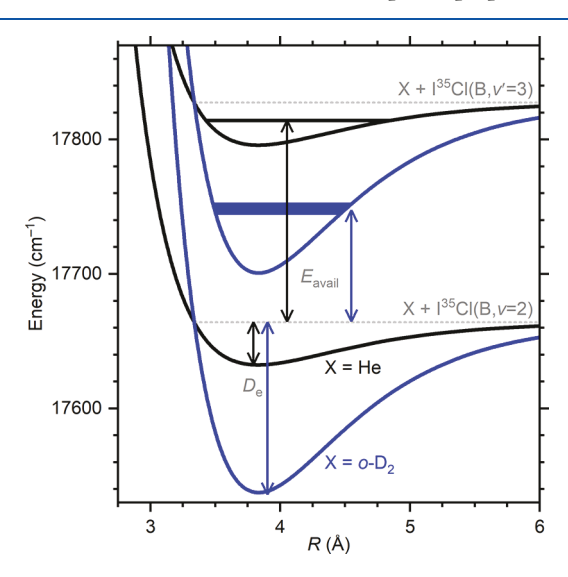


**Figure 3.** Energetics of the VP of the X···l<sup>35</sup>Cl(B, $\nu'=3$ ) complexes to the  $\Delta\nu=-1$  channel with X = o-D<sub>2</sub> (blue) and X = He (black). The potentials were reported previously. <sup>12,32</sup> The initially prepared T-shaped n'=0 X···l<sup>35</sup>Cl(B, $\nu'=3$ ) levels are included in the higher-energy wells, and the amounts of  $E_{\rm avail}$  are shown with arrows. The well depths for the T-shaped orientation,  $D_{\rm e}$ , of the lower-energy potentials are also indicated with arrows.

 $o\text{-}\mathrm{D}_2\cdots I^{35}\mathrm{Cl}(B,\nu'=3,n'=0)$  level results in the dissociating products being closer in energy to the deep well of the lower-energy  $o\text{-}\mathrm{D}_2+I^{35}\mathrm{Cl}(B,\nu=2)$  PES, which has a well depth,  $D_e$ , of  $\sim 130\,$  cm<sup>-1</sup> along the T-shaped geometry. Therefore, the dissociating  $o\text{-}\mathrm{D}_2(j)+I^{35}\mathrm{Cl}(B,\nu=2,j)$  fragments will be affected more by the anisotropy in the well region of that PES as they traverse energetically above it to larger R. In contrast, the T-shaped He···I<sup>35</sup>Cl(B, $\nu'=3,n'=0$ ) complexes have the highest  $E_{\mathrm{avail}}$ , and the He + I<sup>35</sup>Cl(B, $\nu=2,j$ ) VP products exit well above the shallowest of the lower-energy PESs,  $D_e\sim 32\,$  cm<sup>-1</sup>. Thus, for He···I<sup>35</sup>Cl(B, $\nu'=3$ ), the anisotropy of the repulsive region of the PES contributes more to the rotational excitation of the VP

products, and the attributes of the attractive region of the He +  $I^{35}Cl(B, \nu = 2)$  PES contribute less to the rotational excitation.

The relative masses of the complex partners and the conservation of momentum also contribute to the repulsive forces between the two products as they separate from the inner repulsive wall of the lower-energy PES and out the exit channel during the VP of the excited-state complexes. The identical masses of the He and D<sub>2</sub> moieties within the corresponding complexes give rise to the same contributions associated with the conservation of momentum to the product-state distributions. Thus, the warmer  $I^{35}Cl(B_{i}v = 2_{i}j)$  rotational product-state distributions for the D<sub>2</sub>-containing complexes in comparison to the He complex are associated with  $E_{\text{avail}}$ , the well depths, and the anisotropies of the attractive region of the lower-energy PESs sampled during VP. The most likely contributor to the measured differences in the  $I^{35}Cl(B, \nu = 2, j)$  product rotational-state distributions for excitation of the  $p,o-H_2\cdots I^{35}Cl(B,v'=3,n')$  and o,p- $D_2$ ··· $I^{35}Cl(B,v'=3,n')$  complexes is the contrasting masses of the  $H_2$  and  $D_2$  constituents. The lighter mass of the  $H_2$  moiety results in smaller impulsive forces and torque on the  $I^{35}Cl(B, \nu =$ (2,j) fragment as they separate outward toward larger R in comparison to that experienced by the heavier D<sub>2</sub> moiety. This is consistent with the  $I^{35}Cl(B,v=2,j)$   $\langle E_{rot} \rangle$  measured for excitation of the  $p,o-H_2\cdots I^{35}Cl(B,\nu'=3,n')$  levels being significantly lower than those of the  $o_1p-D_2\cdots I^{35}Cl(B_1\nu'=3,n')$  levels and even the He···I<sup>35</sup>Cl(B, $\nu'=3,n'$ ) levels.

The results presented thus far are associated with the  $\Delta \nu = -1$   $I^{35}Cl(B,\nu=2,j)$  VP product rotational-state distributions. Products in the  $\Delta \nu = -2$   $I^{35}Cl(B,\nu=1,j)$  channel were only identified for excitation of the o-D<sub>2</sub>··· $I^{35}Cl(B,\nu'=3,n')$  levels. Excitation spectra collected in the low-energy region of the ICl B–X, 3–0 transition using an expansion of normal-D<sub>2</sub>, including both o-D<sub>2</sub> and p-D<sub>2</sub> with a natural 2:1 abundance, in He are included in Figure 4. The LIF spectrum, Figure 4-top, contains features associated with transitions to the T-shaped o-D<sub>2</sub>···  $I^{35}Cl(B,\nu'=3,n'=0)$  and p-D<sub>2</sub>··· $I^{35}Cl(B,\nu'=3,n'=0)$  levels near 17840 and 17844 cm<sup>-1</sup>, respectively. A much weaker feature associated with the transition to the next higher o-D<sub>2</sub>···  $I^{35}Cl(B,\nu'=3,n'=1)$  level is also observed near 17851 cm<sup>-1</sup>. The  $\Delta \nu = -1$  action spectrum collected with the excitation laser

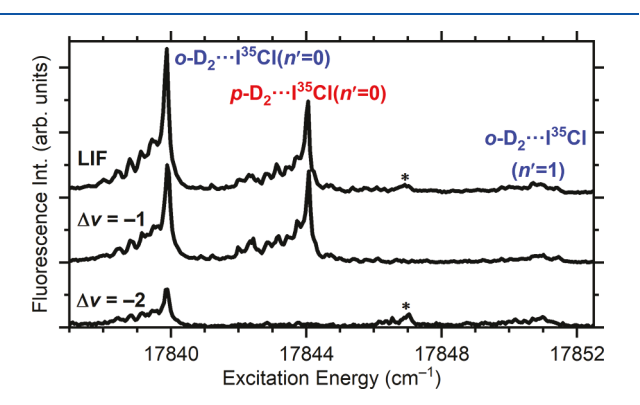


**Figure 4.** Spectra of the T-shaped conformers of o.p-D<sub>2</sub>···I<sup>35</sup>Cl in the ICl B–X, 3–0 region. The upper trace is the laser-induced fluorescence spectrum, the middle and bottom spectra are action spectra recorded by probing the I<sup>35</sup>Cl E–B, 11–2 and 10–1 transitions. The feature near 17851 cm<sup>-1</sup> is associated with the o-D<sub>2</sub>···I<sup>35</sup>Cl complex with one quantum of intermolecular bending excitation, n'=1. The feature marked with an \* is associated with a transition of the linear o-D<sub>2</sub>···I<sup>35</sup>Cl conformer to a delocalized level within the o-D<sub>2</sub> + I<sup>35</sup>Cl(B,v'=2) potential.

scanning through this same spectral region and collecting I<sup>35</sup>Cl E–X emission induced by the probe laser fixed on the rotational bandhead of the I<sup>35</sup>Cl E–B, 11–2 transition is included in Figure 4-middle. The same spectral features are present in this action spectrum as in the LIF spectrum, albeit with different relative intensities, thereby indicating VP products are formed in the  $\Delta \nu$  = -1 D<sub>2</sub> + I<sup>35</sup>Cl(B<sub>1</sub> $\nu$  = 2,j) channel.

The  $\Delta \nu=-2$  action spectrum collected with the probe laser fixed on the bandhead of the I<sup>35</sup>Cl E–B, 10–1 transition, Figure 4-bottom, only contains features associated with transitions to the o-D<sub>2</sub>···I<sup>35</sup>Cl(B, $\nu'=3,n'=0$ ) levels and not to the p-D<sub>2</sub>··· I<sup>35</sup>Cl(B, $\nu'=3,n'=0$ ) level. We attempted to measure the I<sup>35</sup>Cl(B, $\nu=1,j$ ) rotational product-state distribution formed following VP of the o-D<sub>2</sub>···I<sup>35</sup>Cl(B, $\nu'=3,n'=0$ ) level. Unfortunately, the I<sup>35</sup>Cl E–B,  $\nu^{\dagger}-1$  transitions are about an order of magnitude weaker than both the I<sup>35</sup>Cl E–B,  $\nu^{\dagger}-2$  transitions and the I<sup>35</sup>Sl  $\beta$ -A,  $\nu^{\dagger}-\nu$  transitions, which are also present throughout this spectral region. This spectral congestion, as illustrated in Figure S3 in Supporting Information, prohibited the fitting of the I<sup>35</sup>Cl E–B,  $\nu^{\dagger}-1$  features and characterization of the  $\Delta \nu=-2$  I<sup>35</sup>Cl(B, $\nu=1,j$ ) rotational product-state distributions.

The energy-level diagram for the T-shaped  $p,o-H_2\cdots I^{35}$ Cl-(B,v'=3,n'=0) and  $o,p-D_2\cdots I^{35}$ Cl(B,v'=3,n'=0) levels and the energetically accessible product channels, included in Figure 5,

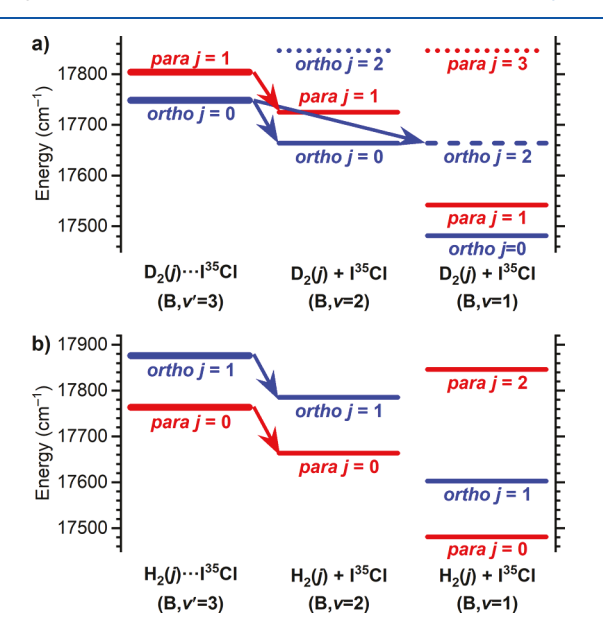


**Figure 5.** Energy-level diagram of the T-shaped  $o_{,p}$ -D<sub>2</sub>···l<sup>35</sup>Cl(B, $\nu'$ =3,n'=0) and  $p_{,o}$ -H<sub>2</sub>···l<sup>35</sup>Cl(B, $\nu'$ =3,n'=0) levels initially prepared (bold lines) and nearby  $o_{,p}$ -D<sub>2</sub> + I<sup>35</sup>Cl(B, $\nu_{,j}$  = 0) and  $p_{,o}$ -H<sub>2</sub> + I<sup>35</sup>Cl(B, $\nu_{,j}$  = 0) product channels are plotted in (a) and (b). The arrows indicate product channels identified. The dashed o-D<sub>2</sub>(j = 2) + I<sup>35</sup>Cl(B, $\nu$  = 1) channel is formed via VP with I<sup>35</sup>Cl(B, $\nu'$ =3) vibrational energy to D<sub>2</sub>(j) rotational energy transfer.

provides insights into the pathway for VP of the o-D<sub>2</sub>··· I<sup>35</sup>Cl(B,v'=3,n'=0,1) levels forming the  $\Delta v$  = -2 I<sup>35</sup>Cl(B,v = 1,j) products. Since the nuclear spins of the H<sub>2</sub>/D<sub>2</sub> molecules cannot change during VP, the p-H<sub>2</sub>/D<sub>2</sub> and o-H<sub>2</sub>/D<sub>2</sub> moieties must remain as para- and ortho-, respectively; in other words, any change in the rotational excitation of the H<sub>2</sub>/D<sub>2</sub> products must follow  $\Delta j$  = 0,  $\pm$  2,  $\pm$  4, ... The  $\Delta v$  = -1 I<sup>35</sup>Cl(B,v = 2,j = 0) product channels that maintain rotational excitation of the H<sub>2</sub>/D<sub>2</sub> moieties,  $\Delta j$  = 0, plotted in Figure 5-center, are the dominant

VP product channels, and they lie just 80 to 100 cm<sup>-1</sup> below the  $p_1o-H_2/D_2\cdots I^{35}Cl(B_1\nu'=3,n'=0)$  levels, left column.

The  $\Delta v = -2 I^{35}Cl(B_i v = 1, j = 0)$  products that also maintain H<sub>2</sub>/D<sub>2</sub> rotational excitation, Figure 5-right, lie much lower in energy, and these are likely not accessed due to energy-gap preferences. The H<sub>2</sub>  $\Delta j$  = +2 channels are not energetically accessible for excitation the  $p,o-H_2\cdots I^{35}Cl(B,v'=3,n')$  levels with low n', Figure 5b. The sole  $H_2/D_2$   $\Delta j = +2$  channel that is energetically open is the o-D<sub>2</sub> $(j = 2) + I^{35}Cl(B, v = 1, j)$  channel, designated by the blue dashed level in Figure 5a-right, and it is nearly isoenergetic with the o-D<sub>2</sub>(j = 0) + I<sup>35</sup>Cl(B, $\nu = 2,j$ ) channel. We conclude the  $\Delta v = -2$  products observed in the action spectrum, Figure 4-bottom, are associated with the o-D<sub>2</sub>...  $I^{35}Cl(B,v'=3,n'=0,\bar{1}) \rightarrow o-D_2(j=2) + I^{35}Cl(B,v=1)$  channel with two quanta of ICl vibrational energy largely converted into the 179.01 cm<sup>-1</sup> of D<sub>2</sub> rotational energy.<sup>34</sup> Angular momentum must also be conserved in this process, but that requires excitation of only a few quanta of  $I^{35}Cl(B, \nu = 1, j)$  rotational excitation since the I35Cl molecular mass is so much larger than the  $D_2$  mass. Rotational excitation up to at least the  $I^{35}Cl(B_1\nu =$ 1,j = 7) state is identified in the probe spectrum, Figure S3 in the Supporting Information.

# CONCLUSIONS

The VP of  $p,o-H_2/D_2\cdots I^{35}Cl(B,v'=3,n')$  intermolecular levels results in similar  $I^{35}Cl(B, \nu = 2, j)$  rotational product-state distributions, and these resemble those measured for excitation of He···I<sup>35</sup>Cl(B, $\nu'$ =3,n') levels. Even though all of the n' = 0 intermolecular vibrational levels are rigidly T-shaped and the excited-state PESs are believed to have comparable anisotropies, there are subtle differences in the  $\Delta \nu = -1 \text{ I}^{35}\text{Cl}(B_i \nu = 2,j)$ rotational product-state distributions. Of the distributions measured for excitation of the lowest-energy, T-shaped n'=0level, the  $p_0$ - $H_2$ ··· $I^{35}$ Cl( $B_1v'=3$ ) complexes are the coldest and the  $o_1p-D_2\cdots I^{35}Cl(B_1\nu'=3)$  complexes are the warmest. Two competing factors are concluded to yield these trends. The o,p- $D_2 \cdots I^{35} Cl(B_1 \nu' = 3_1 n' = 0)$  level is energetically closest to the lower-energy o,p-D<sub>2</sub> +  $I^{35}$ Cl(B, $\nu'$ =2) PES, which has the deepest well of these systems. The departing VP products experience the anisotropy of this well, and the  $I^{35}Cl(B,\nu'=2,j)$  products have higher rotational excitation. The small mass of the H<sub>2</sub> moiety in the  $p_1o-H_2\cdots I^{35}Cl(B_1v'=3,n')$  levels results in less momentum transfer to the I35Cl molecule and a colder distribution in comparison to the o,p- $D_2$ ··· $I^{35}$ Cl(B,v'=3,n') levels. The preparation of levels with intermolecular bending excitation that sample the linear regions of the PES yields colder  $\Delta \nu = -1$ rotational product-state distributions for all of the complexes. There are no identifiable trends in the distributions that can be associated with the different hydrogen rotational excitation, para- versus ortho-hydrogen, within the excited-state complexes. This suggests the stronger intermolecular interactions and higher binding energies for the j = 1 hydrogen state than the j = 0state with ICl do not play significant roles in VP as the repulsive regions of the PESs accessed are well above the well of the lowerenergy surface. Comparisons of the  $\Delta v = -1$  product-state distributions obtained for excitation of the  $D_2 \cdots I^{35}Cl(B_1 \nu' = 3_1 n')$ and He···I<sup>35</sup>Cl(B, $\nu'$ =3,n') levels permit the roles of the mass of the complex partners, and the well depths, of the lower-lying PESs to be separated. As the masses of the complex partners are the same for these two systems, the slightly warmer  $I^{35}Cl(B_{\nu} =$ 2,j) rotational product-state distributions measured for the deuterium complexes are associated with their significantly smaller amount of  $E_{\text{avail}}$  and the resultant sensitivity to the

attractive well of the lower-lying PES. Lastly, the o-D $_2$ ···  $I^{35}$ Cl(B, $\nu'$ =3,n'=0,1) levels are observed to undergo VP with efficient ICl vibrational to D $_2$  rotational-energy transfer with almost 70% of the available energy being imparted to the D $_2$  rotation.

#### ASSOCIATED CONTENT

# Supporting Information

The Supporting Information is available free of charge at https://pubs.acs.org/doi/10.1021/acs.jpca.2c05817.

Fits of rotational product-state spectra, scheme for subtracting continuum features, and  $\Delta \nu = -2$  rotational product spectra of  $o\text{-}\mathrm{D}_2\cdots\mathrm{I}^{35}\mathrm{Cl}(B,\nu'=3,n'=0)$  (PDF)

# AUTHOR INFORMATION

# **Corresponding Authors**

Joshua P. Darr — Department of Chemistry, University of Nebraska at Omaha, Omaha, Nebraska 68182, United States; orcid.org/0000-0003-4704-357X; Email: jdarr@unomaha.edu

Richard A. Loomis — Department of Chemistry, Washington University in St. Louis, Saint Louis, Missouri 63130, United States; orcid.org/0000-0002-3172-6336; Email: loomis@wustl.edu

Complete contact information is available at: https://pubs.acs.org/10.1021/acs.jpca.2c05817

#### **Notes**

The authors declare no competing financial interest.

# ACKNOWLEDGMENTS

This work was partially supported by the NSF under grant CSDMA-2102241. Acknowledgment is made to the donors of the American Chemical Society Petroleum Research Fund for partial support of this research.

### REFERENCES

- (1) Levy, D. H. Van der Waals molecules. *Adv. Chem. Phys.* **1981**, *47*, 323.
- (2) Rohrbacher, A.; Halberstadt, N.; Janda, K. C. The dynamics of noble gas-halogen molecules and clusters. *Annu. Rev. Phys. Chem.* **2000**, *51*, 405.
- (3) Rohrbacher, A.; Williams, J.; Janda, K. C. Rare gas-dihalogen potential energy surfaces. *Phys. Chem. Chem. Phys.* **1999**, *1*, 5263.
- (4) Drobits, J. C.; Skene, J. M.; Lester, M. I. Direct lifetime and nascent product distribution for the vibrational predissociation of ICl-Ne  $A(^{3}\Pi_{1})$  state van der Waals complexes. *J. Chem. Phys.* **1986**, *84*, 2896.
- (5) Skene, J. M.; Drobits, J. C.; Lester, M. I. Dynamical effects in the vibrational predissociation of ICl-rare gas complexes. *J. Chem. Phys.* **1986**, 85, 2329.
- (6) Waterland, R. L.; Lester, M. I.; Halberstadt, N. Quantum dynamical calculations for the vibrational predissociation of the heliumiodine chloride (He-ICl) complex: product rotational distribution. *J. Chem. Phys.* **1990**, *92*, 4261.
- (7) Waterland, R. L.; Skene, J. M.; Lester, M. I. Rotational rainbows in the vibrational predissociation of ICl-He complexes. *J. Chem. Phys.* **1988**, *89*, 7277.
- (8) Cline, J. I.; Reid, B. P.; Evard, D. D.; Sivakumar, N.; Halberstadt, N.; Janda, K. C. State-to-state vibrational predissociation dynamics and spectroscopy of HeCl<sub>2</sub>: Experiment and theory. *J. Chem. Phys.* **1988**, *89*, 3535.
- (9) Darr, J. P.; Loomis, R. A.; McCoy, A. B. The dissociation dynamics of  $\text{He}{}\cdots\text{I}^{35}\text{Cl}(B, \nu'=2,3)$  complexes with varying amounts of internal energy. *J. Chem. Phys.* **2005**, *122*, 044318.

- (10) Boucher, D. S.; Loomis, R. A. Stabilization of different conformers of weakly bound complexes to access varying excited-state intermolecular dynamics. *Adv. Chem. Phys.* **2008**, *138*, 375.
- (11) Darr, J. P.; Crowther, A. C.; Loomis, R. A.; Ray, S. E.; McCoy, A. B. Probing the dependence of long-range, four-atom interactions on intermolecular orientation. 1. Molecular hydrogen and iodine monochloride. *J. Phys. Chem. A* **2007**, *111*, 13387.
- (12) Darr, J. P.; Loomis, R. A.; McCoy, A. B. Probing the dependence of long-range, four-atom interactions on intermolecular orientation: 2. Molecular deuterium and iodine monochloride. *J. Phys. Chem. A* **2008**, 112, 9494.
- (13) Darr, J. P.; Loomis, R. A.; Ray-Helmus, S. E.; McCoy, A. B. Probing the dependence of long-range, four-atom interactions on intermolecular orientation: 3. Hydrogen and iodine. *J. Phys. Chem. A* **2011**, *115*, 7368.
- (14) Boucher, D. S.; Strasfeld, D. B.; Loomis, R. A.; Herbert, J. M.; Ray, S. E.; McCoy, A. B. Stabilization and rovibronic spectra of the T-shaped and linear ground-state conformers of a weakly bound rare-gashomonuclear dihalogen complex: He···Br<sub>2</sub>. *J. Chem. Phys.* **2005**, *123*, 104312
- (15) Bradke, M. D.; Loomis, R. A. Spectroscopic observation of the preferentially stabilized, linear He···ICl(X  $^{1}\Sigma^{+}$ ) complex. *J. Chem. Phys.* **2003**, *118*, 7233.
- (16) Burke, M. L.; Klemperer, W. The one-atom cage effect: Continuum processes in molecular iodine-argon ( $I_2$ -Ar) below the B-state dissociation limit. *J. Chem. Phys.* **1993**, *98*, 1797.
- (17) Higgins, K.; Tao, F.-M.; Klemperer, W. The intermolecular potential between an inert gas and a halogen: Prediction and observation of transitions between the linear and T-shaped isomers of HeClF. *J. Chem. Phys.* **1998**, *109*, 3048.
- (18) Ray, S. E.; McCoy, A. B.; Glennon, J. J.; Darr, J. P.; Fesser, E. J.; Lancaster, J. R.; Loomis, R. A. Experimental and theoretical investigations of the He···I<sub>2</sub> rovibronic spectra in the I<sub>2</sub> B-X, 20–0 region. J. Chem. Phys. **2006**, 125, 164314.
- (19) Strasfeld, D. B.; Darr, J. P.; Loomis, R. A. Experimental characterization of the Ne + ICl(X, v''=0) and Ne + ICl(X, v''=2) multidimensional intermolecular potentials. *Chem. Phys. Lett.* **2004**, 397, 116
- (20) Boucher, D. S.; Darr, J. P.; Bradke, M. D.; Loomis, R. A.; McCoy, A. B. A combined experimental/theoretical investigation of the He + ICl interactions: Determination of the binding energies of the T-shaped and linear He···I<sup>35</sup>Cl(X,  $\nu''$ =0) conformers. *Phys. Chem. Chem. Phys.* **2004**, *6*, 5275.
- (21) Gordon, R. D.; Innes, K. K. Predissociation in the  $B^3\Pi_{0+}$  state of  $I^{35}Cl$  and  $I^{37}Cl$ . J. Chem. Phys. 1979, 71, 2824.
- (22) Olson, C. D.; Innes, K. K. Sing-rotational-level lifetimes from measurements of linewidths in the B  $^3\Pi_{0+} \leftarrow X$   $^1\Sigma^+$  system of ICl\*. *J. Chem. Phys.* **1976**, *64*, 2405.
- (23) Suzuki, T.; Kasuya, T. Predissociative lifetimes of single rovibronic levels of the B  $^3\Pi_{0+}(v'=3)$  state of ICl. *J. Chem. Phys.* **1984**, *81*, 4818.
- (24) Darr, J. P.; Loomis, R. A. Experimental interrogation of the multidimensional He + ICl(E,  $v^{\dagger}$ ) and He + ICl( $\beta$ ,  $v^{\dagger}$ ) intermolecular potential energy surfaces. *J. Chem. Phys.* **2008**, *129*, 144306.
- (25) Brand, J. C. D.; Deshpande, U. D.; Hoy, A. R.; Jaywant, S. M. Polarization spectroscopy of ion-pair states of ICl. *J. Mol. Spectrosc.* **1983**, *100*, 416.
- (26) Bussières, D.; Hoy, A. R. The three lowest ion-pair states of ICl. Can. J. Phys. 1984, 62, 1941.
- (27) Takei, T.-A.; Watanabe, A.; Amako, Y. Spectroscopic constants for the B  $^3\Pi_{0+}$  state of I  $^{35}$ Cl and for the B  $^3\Pi_{0+}$  and B′  $^0$  states of I  $^{37}$ Cl. *J. Mol. Spectrosc.* **1995**, *171*, 287.
- (28) Darr, J. P.; Crowther, A. C.; Loomis, R. A. Direct measurement of the binding energy of the linear He···I<sup>35,37</sup>Cl(X) isotopomers. *Chem. Phys. Lett.* **2003**, 378, 359.
- (29) Darr, J. P.; Glennon, J. J.; Loomis, R. A. Observation of bound-free transitions of the linear Ar···I<sub>2</sub>(X,  $\nu''$ =0) complex in and above the I<sub>2</sub> B-X spectral region. J. Chem. Phys. **2005**, 122, 131101.

- (30) Pio, J. M.; van der Veer, W. E.; Bieler, C. R.; Janda, K. C. Product state resolved excitation spectroscopy of He-, Ne-, and Ar-Br<sub>2</sub> linear isomers: Experiment and theory. *J. Chem. Phys.* **2008**, *128*, 134311.
- (31) Cabrera, J. A.; Bieler, C. R.; Olbricht, B. C.; van der Veer, W. E.; Janda, K. C. Time dependent pump-probe spectra of NeBr<sub>2</sub>. *J. Chem. Phys.* **2005**, *123*, 054311.
- (32) McCoy, A. B.; Darr, J. P.; Boucher, D. S.; Winter, P. R.; Bradke, M. D.; Loomis, R. A. A combined experimental/theoretical investigation of the He + ICl interactions: I. The ro-vibronic spectrum of He···ICl complexes in the ICl *B-X*, 3–0 region. *J. Chem. Phys.* **2004**, 120. 2677.
- (33) Nejad-Sattari, M.; Stephenson, T. A. Fragment rotational distributions from the dissociation of NeBr<sub>2</sub>: Experimental and classical trajectory studies. *J. Chem. Phys.* **1997**, *106*, 5454.
- (34) Bredohl, H.; Herzberg, G. The Lyman and Werner bands of deuterium. Can. J. Phys. 1973, 51, 867.